

1 Visible Light Plasmon Excitation of Silver

2 Nanoparticles Against Antibiotic-Resistant

3 *Pseudomonas aeruginosa*

4 Rafael T. P. da Silva^{a,*}, Marcos V. Petri^{a,*}, Estela Y. Valencia^{b,*}, Pedro H. C. Camargo^{a,c},

5 Susana I. C. de Torresi^a, Beny Spira^{b,#}

6 AUTHORS ADDRESSES

7 ^aDepartment of Fundamental Chemistry, Institute of Chemistry, University of São Paulo,

8 Brazil

9 ^bDepartment of Microbiology, Institute of Biomedical Sciences, University of São Paulo,

10 Brazil

11 ^cDepartment of Chemistry, Faculty of Science, University of Helsinki, Finland

12

13 # Address correspondence to Beny Spira, benys@usp.br

14 *Rafael T. P. da Silva, Marcos V. Petri and Estela Y. Valencia contributed equally to this
15 work. Author order was determined by consensual agreement.

16

17 ABSTRACT

18 The interaction of metallic nanoparticles with light excites a local surface plasmon resonance
19 (LSPR). This phenomenon enables the transfer of hot electrons to substrates that release
20 Reactive Oxygen Species (ROS). In this context, the present study was aimed at enhancing
21 the antibacterial effect of citrate-covered silver nanoparticles (AgNPs), which already possess
22 excellent antimicrobial properties, via LSPR excitation with visible LED
23 against *Pseudomonas aeruginosa*, one of the most refractory organisms to antibiotic

24 treatment. The Minimum Inhibitory Concentration (MIC) of AgNPs was 10 µg/ml under dark
25 conditions and 5 µg/ml under light conditions. The combination of light and AgNPs led to
26 100% cell death after 60 minutes. Quantification of ROS via flow cytometry showed that
27 LSPR stimulated AgNPs increased intracellular ROS concentration by 4.8-fold, suggesting
28 that light-exposed AgNPs caused cell death via ROS production. Light exposition caused a
29 small release of silver ions (0.4%) reaching a maximum after 6 hours. This indicates that
30 silver ions play at most a secondary role in *P. aeruginosa* death. Overall, the results presented
31 here show that LSPR generation from AgNPs by visible light enhances the antimicrobial
32 activity of silver nanoparticles and can be an alternative for the treatment of topic infections
33 caused by antibiotic-resistant bacteria such as *P. aeruginosa*.

34

35 KEYWORDS: Silver nanoparticles, Surface Plasmon resonance, *Pseudomonas aeruginosa*,
36 Antibiotic resistance

37

38 **Running title:** Light-enhanced Ag nanoparticles against *P. aeruginosa*

39

40

41 **Introduction**

42 Metallic nanoparticle possess remarkable features, such as their manageable scale and the
43 ability of fine tuning their composition, structure and shape (1). The desired electronic,
44 optical and chemical properties of nanoparticles can be obtained through modern synthetic
45 techniques devised in the past decades (2). Even small variations in one of these parameters
46 may result in new properties that are absent in the analogous bulk material. Due to its high
47 range of controllable features, metallic nanoparticles are now used in many processes, such as

48 catalysis (3), SERS (4), electroanalytical sensors (5), plasmonics (6), photonics (7) and
49 others.

50 Silver nanoparticles (AgNPs)(2), exhibit a great potential of use in many areas, due to their
51 relative easy and controlled synthesis (8), ranging from small and simple spheroidal AgNPs
52 (9) to more complex geometries (10, 11) and even asymmetric shapes (12–14) with solid or
53 hollow interiors (15–17). Historically, silver has been extensively used as an antimicrobial
54 agent. Many different commercial products relying on silver biocidal properties have been
55 produced, most of them in the last 10 years (18, 19). The wide variety of AgNPs as well as
56 the intrinsic properties of metallic silver in relation to biological system and biomolecules
57 (20) fostered the extensive use of AgNPs in medical applications, such as cancer treatment
58 (21–23), drug delivery (24, 25), imaging (26, 27) and antimicrobial treatment (28, 29).

59 *P. aeruginosa* is a ubiquitous Gram-negative γ -proteobacterium and an opportunistic
60 pathogen associated with nosocomial infections. It also affects patients afflicted by chronic
61 respiratory diseases such as cystic fibrosis (30, 31). The relatively large genome and genetic
62 complexity of *P. aeruginosa* (32, 33) supports its versatility and ability to colonize the soil,
63 water bodies, as well as plants and animal tissues (33). *P. aeruginosa* infections are
64 frequently refractory to quinolone, aminoglycosides and β -lactam antibiotics (34). In fact,
65 owe to its outer membrane low permeability, expression of efflux pumps, and biofilm
66 formation, *P. aeruginosa* is one of the most difficult organisms to treat with antibiotics. Skin
67 infections by *P. aeruginosa* on burn victims are particularly problematic, in part due to non-
68 efficient treatments (35–37). The World Health Organization (WHO) included carbapenem
69 resistant *P. aeruginosa* in a list of critical priority bacteria to which the research and
70 development of new antibiotics and alternative treatments is of paramount importance (38).

71 Although anti-bacterial treatments with visible light, such as blue light therapy (BLT) have
72 been emerging as a non-invasive treatment for bacterial infections, the interaction of visible

73 light with AgNPs in the range of LSPR and its possible effect on microbes has not yet been
74 studied (39). Inspired by these findings, in the present work we use the concept of LSPR in
75 order to enhance the antimicrobial properties of AgNPs against *P. aeruginosa* by illuminating
76 the system with a white LED lamp. This strategy revealed a quicker and more effective
77 treatment against *P. aeruginosa*, being a promising improvement in the fight against this
78 pathogen.

79

80 **Results and Discussion**

81 **AgNPs synthesis**

82 Citrate covered AgNPs have been widely used in biological applications. Citrate, a natural
83 anti-oxidant is not harmful to cells and is used as a carbon source by some bacteria. We
84 synthesized citrate-covered AgNPs with a diameter of 20 ± 3 nm (Figure 1a). The extinction
85 spectrum displayed a full width at half maximum (FWHM) of 131 nm and a maximum at 436
86 nm, a wavelength that matches the maximum emission from the LED floodlight used here
87 (Figure 1b). The extinction band is broadened due to the standard deviation in particle size
88 distribution, which represents ca. 15% of the average diameter. This is a typical spectrum for
89 AgNPs synthesized by the citrate method (40, 41). In order to optimally observe the effects of
90 the LSPR phenomenon, the excitation of AgNPs with an external radiation source should be
91 performed in the region of maximum absorption. Therefore, a floodlight with an emission
92 spectrum that superposes the AgNPs extinction spectrum was utilized (Figure 1b). To avoid
93 the mutagenic and carcinogenic effects of UV light, a light source that did not emit in the UV
94 region was chosen.

95

96 **Bactericidal effect of AgNPs on *P. aeruginosa***

97 Preliminary assays showed that the synthesized AgNPs displayed antimicrobial activity
98 against *P. aeruginosa*. The minimal inhibitory concentration (MIC) of AgNPs was 10 µg/mL,
99 which is comparable to values reported by similar studies for the same bacterium(42–44).
100 However, when the AgNPs were exposed to light the MIC dropped to 5 µg/mL. The minimal
101 bactericidal concentrations (MBC) were 20 µg/mL and 10 µg/mL under dark and light
102 conditions, respectively. In addition, a Kirby-Bauer assay using filters containing different
103 concentrations of AgNPs was performed in the presence and absence of light (Fig. 2). In the
104 absence of light (Fig. 2A), an inhibition halo became apparent with AgNPs concentrations
105 higher than 15 µg/mL and larger halos were observed with AgNPs concentrations up to 30
106 µg/mL. In contrast, when the AgNPs were exposed to light, 10 µg/mL sufficed to produce a
107 halo similar to that observed when the bacteria were treated with 30 µg/mL AgNPs in the
108 dark, suggesting that light enhances the bactericidal effect of silver nanoparticles (Figure 2B).
109

110 It is worth noticing that upon light exposition, the greenish color of *P. aeruginosa* colonies,
111 caused by the synthesis of the pigments pyoverdine and pyocyanin visually decrease. These
112 molecules are well-known virulence factors of *P. aeruginosa* are targets for the screening of
113 antimicrobial compounds (45–47). Accordingly, some studies have shown that light reduces
114 the concentration of pyocyanin in *P. aeruginosa* and that this effect was dependent on light
115 intensity and wavelength (48). It has also been shown that high doses of blue light treatment
116 inhibited the activity of pyocyanin, staphylolysin, pseudolysin and other proteases (37, 39).
117 Furthermore, it has been demonstrated that pyocyanin confers on *P. aeruginosa* resistance to
118 ionic silver (49). It is thus possible that pyocyanin inhibition by LED floodlight contributes to
119 the bactericidal effect of AgNPs on *P. aeruginosa* and diminishes the virulence of the
120 surviving bacteria.

121 To further explore the effect of light exposition on *P. aeruginosa*, bacteria were grown for 60
122 minutes in MH medium without AgNPs in the presence or absence of light (Fig. 6). The
123 calculated growth rates were 1.26 h^{-1} and 1.04 h^{-1} under dark and light conditions,
124 respectively, a 17.5% reduction, suggesting that light mildly affects bacterial growth.

125 Next, we measured the effect of AgNPs on cell viability at different time intervals. Bacteria
126 treated for 15, 30 and 60 minutes with 1X MIC AgNPs showed a survival rate of 12.8%,
127 4.4% and 1.6% in the dark and 4.5%, 0.7% and 0.2% under light conditions, respectively
128 (Fig. 3a), while bacteria treated with 2X MIC showed, respectively, a survival rate of 20.6%,
129 6.4% and 2.2% (dark conditons) and 3.6%, 0.4% and 0.0% (light conditions) at 15, 30 and 60
130 minutes (Fig. 3b). An 1 h treatment with 10 or 20 $\mu\text{g/mL}$ AgNPs under light exposition
131 resulted in 99.8% and 100% cell death, respectively. These results corroborate the
132 bactericidal effect of AgNPs on *P. aeruginosa* and the enhancing effect of light exposure
133 upon AgNPs treatment.

134

135 **Effect of light and AgNPs on ROS generation**

136 The antimicrobial mechanism of action of AgNPs is still not fully understood mainly due to
137 the difficulty in evaluating the contributions of nanosized metallic silver and silver ions that
138 are released by the former (50, 51). While some studies support the idea that silver ions play
139 the main role in cellular damage (52), others claim that the strong antibacterial activity of
140 AgNPs is associated with the introduction of nicks in the cytoplasmic membrane which
141 ultimately lead to cell death (53). In addition, AgNPs (and silver ions) induce the formation
142 of reactive oxygen species (ROS) (54), which damage the cell cytoskeleton, and oxidize
143 proteins and nucleic acids, potentially leading to chromosomal aberrations and cell demise.
144 Also, both ionic and nanosized silver can interact with sulphur-containing macromolecules,

145 such as proteins, resulting in their inactivation (55). Lately, a Trojan-horse like mechanism
146 has been proposed, in which AgNPs first enter the cell and only then release silver ions (56).
147 Previous studies showed that AgNPs promote the induction of reactive oxygen species (ROS)
148 (57, 58) and enhance the expression of superoxide dismutase, catalase and peroxidase (58).
149 These authors concluded that the main mechanism of antimicrobial action of AgNPs involves
150 the disequilibrium of oxidation and antioxidation processes and the inability to eliminate
151 ROS (58). High concentration of ROS in the bacterium lead to oxidative stress (59, 60). To
152 test whether AgNPs causes oxidative stress, the intracellular level of ROS in *P. aeruginosa*
153 was assessed. Bacteria were treated with 1X MIC AgNPs under light or dark conditions
154 followed by exposure to 2',7'-Dichlorofluorescein diacetate (DCFH-DA). This compound
155 diffuses into the cell where it is hydrolyzed by intracellular esterases (DCFH), resulting in the
156 production of 2',7'-dichlorofluorescein (DCF), which fluoresces upon oxidation. The
157 intracellular ROS level thus correlates with the level of fluorescence emitted by DCF in the
158 presence of ROS such as H_2O_2 , ROO^- and $ONOO^-$ (61). Fig. 4 shows that after 1 hour in the
159 presence of AgNPs, the level of ROS increased by 2.5-fold (dark) and 4.8-fold (light) when
160 compared to the respective controls.

161 In a conducting medium, surface electrons of nanoparticles may oscillate in a resonant
162 condition with a coupled electromagnetic field, resulting in a phenomenon called Local
163 Surface Plasmon Resonance (LSPR), which confer on nanoparticles physical unique
164 properties. Among them, a local temperature increase, enhancement of optical near fields
165 surrounding the particle and the generation of hot carriers can be highlighted (62). The last
166 one received a special attention in the field of catalysis due to the possibility of electronic or
167 vibrational activation of substrates or reaction intermediates. Interestingly, recent studies
168 have demonstrated the formation of ROS at the surface of metallic nanoparticles (63–65). For

169 example, LSPR-based antibacterial treatment with gold nanoparticles has been reported (66–
170 68).

171 It has been suggested that the formation of ROS by AgNPs occurs either at the particle
172 surface or it is indirectly caused by Ag^+ ions released from aging nanoparticles (69, 70). In
173 addition, the light stimulus may contribute to the amount of ROS generated through a
174 mechanism of plasmon-produced hot electrons and their interaction with water and oxygen
175 dissolved in the medium (63–65). To assess whether exposure to light affects the production
176 of Ag^+ from AgNPs by an aging process, a closed dialysis membrane filled with an AgNPs
177 suspension was submerged in distilled water and the concentration of released Ag^+ to the
178 solution was followed during 24 h (Fig. 5). At 0 h the concentration of silver ions was below
179 the limit of detection of ICP-OES. The highest concentration of Ag^+ under dark conditions
180 was four times lower than that observed under light exposition. Although the concentration of
181 Ag^+ increased with light treatment, the highest observed concentration (at 6 h, under light
182 exposition) represented only 0.4% (w/w) of the total amount of silver in the sample.
183 Moreover, the release of Ag^+ occurred several hours after AgNPs have already killed the
184 bacteria (see Fig. 3) . At the time in which the bactericidal effect and ROS were evaluated (1
185 h), it is noticeable that the measured concentrations of Ag^+ under light and dark conditions
186 are statistically indistinguishable. Therefore, the release of Ag^+ is unlikely to be involved in
187 the mechanism through which AgNPs cause bacterial death.

188

189 **Conclusion**

190 AgNPs were shown to be effective against *P. aeruginosa*. The bactericidal effect of AgNPs
191 were intensified when the system was irradiated by light, indicating that the combination of
192 light and AgNPs ensures a quick and more effective treatment against this pathogen. A
193 treatment period of one hour was sufficient to cause complete cell death. These effects were

194 associated with an increase in intracellular ROS possibly generated by the hot carrier transfer
195 of LSPR on the AgNPs surface. AgNPs aging and the consequent release of silver ions
196 occurred only after long periods of exposition to light. Our data illustrate a viable treatment
197 that combines two pre-existing strategies: the use of both AgNPs and light treatment, that
198 synergistically enhance the treatment of *P. aeruginosa* topical infections.

199

200 **Materials and Methods**

201 **Materials**

202 Silver nitrate (AgNO_3 , Sigma-Aldrich, $\geq 99\%$), sodium citrate (Sigma-Aldrich, $\geq 99\%$),
203 lysogeny broth medium (KASVI, Curitiba, Brazil), phosphate buffer saline (PBS, pH 7.4),
204 bacteriological agar (KASVI, Curitiba, Brazil), Mueller-Hinton broth (BD Difco) and 2',7'-
205 dichlorofluorescein diacetate (DCFH-DA, $\geq 97\%$, Sigma-Aldrich) were of analytical grade and
206 used as received. All solutions were prepared using deionized water (18.2 M Ω) unless stated
207 otherwise. Sterile filter paper discs of 6 mm, 96-well flat bottom plates (Corning) and 24-well
208 flat bottom plates (Corning) were used as received.

209

210 **Synthesis of Silver Nanoparticles (AgNPs)**

211 Preparation of AgNPs followed a slightly modified method of Lee and Meisel (71). AgNO_3
212 (90 mg) was dissolved in 500 mL of distilled water. The solution was heated until boiling
213 under magnetic stirring. Ten mL of a 34 mM sodium citrate solution were then added and the
214 mixing which proceeded for another 1 hour. The suspension was transferred to an amber
215 flask and stored at room temperature until further use.

216

217 **Sample preparation for electron microscopy (SEM and TEM)**

218 One mL of the as synthesized AgNPs suspension was washed three times by successive
219 rounds of centrifugation at 17000 rpm. The pellet containing the AgNPs was resuspended in
220 20 μ L or 300 μ L of water. For the SEM analysis, 1 μ L of the concentrated suspension was
221 deposited onto a 1 cm^2 silicon wafer and let dry at room temperature. For the TEM analysis,
222 10 μ L of the suspension was transferred to a standard formvar coated copper TEM grid and
223 dried at room temperature. Particles size were analysed with the help of the ImageJ 2.0
224 software.

225

226 **Media and bacterial growth conditions**

227 *Pseudomonas aeruginosa* (strain PA14) was typically cultivated in LB medium at 37°C for
228 16 h. The culture was then diluted 1/100 in 5 mL of MH, and grown until the exponential
229 growth phase ($\text{OD}_{600} = 0.1$). Mueller-Hinton agar plates (MHA-DIFCO) were used in the
230 bacterial viability assays in solid medium. Bacterial growth rate was determined by growing
231 cells under dark or light conditions in MH medium and measuring the number of colony
232 forming units (CFU/mL) at different time points.

233

234 **Determination of the minimum inhibitory concentration (MIC)**

235 MIC determination was performed by the broth microdilution technique (Clinical and
236 Laboratory Standards Institute – CLSI, 2015). Briefly, 10^5 bacteria/ml were inoculated in 96-
237 well plates containing Mueller-Hinton medium and incubated in the presence of increasing
238 concentrations of AgNPs (from 0 to 80 $\mu\text{g/mL}$). One plate was covered with aluminium foil
239 (dark conditions) and the other was placed on the top of it (light conditions). The plate on the
240 top was positioned 10 cm away from a LED floodlight (50 W). Both plates were incubated
241 overnight at 30°C. On the next day the turbidity of the cultures was measured at 600 nm in an
242 EpochTM Microplate Spectrophotometer (BioTek).

243

244 **Antimicrobial activity of AgNPs (disc diffusion method)**

245 The antimicrobial activity of AgNPs in solid medium was evaluated through the Kirby-Bauer
246 disc diffusion method according to the guidelines provided (Clinical and Laboratory
247 Standards Institute – CLSI, 2015). Mueller-Hinton agar plates were evenly swabbed with 100
248 μL of a PA14 culture ($\text{OD}_{600} = 0.1$). Sterile filter paper discs (6 mm diameter, Oxoid) were
249 uniformly placed on the plate surface and 10 μL of different concentrations of AgNPs were
250 dropped onto each disc. The negative control was sodium citrate at the same concentration of
251 the AgNPs suspension. Plates were incubated overnight at 30 °C and the halos formed by
252 antibiotic activity against the bacteria were measured with the help of the ImageJ 2.0
253 software.

254

255 **Kinetics of AgNPs antibacterial effect**

256 Two 24-well plates were filled with 1.5 mL of a mixture of MH medium and AgNPs (0, 1X
257 and 2X MIC). A final concentration of 10^5 cells/mL at the exponential growth phase was
258 added to each well. One of the plates was covered with aluminium foil (dark conditions) and
259 the other one was placed on its top (light conditions). Both plates were statically incubated at
260 30°C, while the plate on the top was 10 cm away from a LED floodlight (50 W). Aliquots of
261 100 μL were withdrawn at 0, 15, 30 and 60 minutes from both plates and subsequently
262 diluted in 0.9% NaCl, plated on LB-Agar and incubated for 24 h at 37 °C. The number of
263 colony forming units (CFU/mL) was determined. This experiment was performed with
264 twelve biological replicates.

265

266 **Intracellular ROS assay**

267 Three independent overnight cultures of *P. aeruginosa* were diluted 1:100 in fresh MH
268 medium, incubated under agitation until reaching the concentration of 10^8 cells/mL. Different
269 concentrations of AgNPs and 20 μ M DCFH-DA were then added. The cultures were
270 incubated at 30 °C for 1h in the presence and absence of light exposition. Then, 1 mL of each
271 culture was withdrawn and centrifuged at 8000 rpm for 5 minutes. The pellets were washed
272 with 1 mL of PBS and suspended again in 100 μ L of PBS. The fluorescence emitted by the
273 intracellular oxidation of the dye was determined using the BD AccuriTM C6 flow cytometer
274 at the excitation wavelength of 488 nm and at an emission wavelength of 535 nm.

275

276 **Quantification of released Ag⁺**

277 Six dialysis membranes each filled with 20 mL AgNPs were placed in 800 mL beakers filled
278 with 500 mL distilled water under magnetic stirring. Three of them were placed 10 cm away
279 from the floodlight, while the other three were covered in aluminium foil. After 1, 2, 4, 6 and
280 24 h, 5 mL aliquots of water from each beaker were withdrawn and stored for further
281 analysis. Silver ions were detected by iCAPTM 7000 Plus Series ICP-OES (Thermo
282 ScientificTM).

283

284 **Statistical**

285 Statistical significance was calculated using the analysis of variance (ANOVA) followed by
286 Tukey pairwise comparison. Values of $p \leq 0.05$ were considered statistically significant.

287

288 **Acknowledgments**

289 This work was supported by FAPESP (grant number 2018/13492-2; 2015/26308-7). E.Y.V
290 was funded by a postdoctoral fellowship from PNPd/CAPES (grant 1680341). R.T.P.S was
291 funded by a PhD fellowship from CAPES (grant 88882.328241/2019-01).

292

293 **References**

- 294 1. Lim B, Wang J, Camargo PHC, Cobley CM, Kim MJ, Xia Y. 2009. Twin-Induced Growth of
295 Palladium-Platinum Alloy Nanocrystals. *Angew CHEMIE-INTERNATIONAL* Ed 48:6304–6308.
- 296 2. Sun Y. 2002. Shape-Controlled Synthesis of Gold and Silver Nanoparticles. *Science* (80-)
297 298:2176–2179.
- 298 3. Wang J, Barbosa ECM, Fang Z, Parussulo ALA, Reis FVE, Ando RA, Araki K, Toma HE,
299 Camargo PHC. 2018. On the effect of TiO₂ nanocrystallites over the plasmonic photodegradation by
300 Au nanoparticles. *J Raman Spectrosc* 49:1953–1960.
- 301 4. Haldavnekar R, Venkatakrishnan K, Tan B. 2018. Non plasmonic semiconductor quantum
302 SERS probe as a pathway for in vitro cancer detection. *Nat Commun* 9:3065.
- 303 5. Dourado AHB, da Silva AGM, Pastroián FAC, Munhos RL, de Lima Batista AP, de Oliveira-
304 Filho AGS, Quiroz J, de Oliveira DC, Camargo PHC, Córdoba de Torresi SI. 2019. In situ FTIR
305 insights into the electrooxidation mechanism of glucose as a function of the surface facets of Cu₂O-
306 based electrocatalytic sensors. *J Catal* 375:95–103.
- 307 6. Geonmonond RS, da Silva AGM, Rodrigues TS, de Freitas IC, Ando RA, Alves T V.,
308 Camargo PHC. 2018. Addressing the Effects of Size-dependent Absorption, Scattering, and Near-
309 field Enhancements in Plasmonic Catalysis. *ChemCatChem* 10:3447–3452.
- 310 7. Sun L, Lin H, Kohlstedt KL, Schatz GC, Mirkin CA. 2018. Design principles for photonic
311 crystals based on plasmonic nanoparticle superlattices. *Proc Natl Acad Sci* 115:7242–7247.
- 312 8. da Silva AGM, Rodrigues TS, Haigh SJ, Camargo PHC. 2017. Galvanic replacement
313 reaction: recent developments for engineering metal nanostructures towards catalytic applications.
314 *Chem Commun* 53:7135–7148.
- 315 9. Bastús NG, Merkoçi F, Piella J, Puntès V. 2014. Synthesis of Highly Monodisperse Citrate-
316 Stabilized Silver Nanoparticles of up to 200 nm: Kinetic Control and Catalytic Properties. *Chem*
317 *Mater* 26:2836–2846.
- 318 10. Wang Y, Wan D, Xie S, Xia X, Huang CZ, Xia Y. 2013. Synthesis of Silver Octahedra with

- 319 Controlled Sizes and Optical Properties via Seed-Mediated Growth. ACS Nano 7:4586–4594.
- 320 11. Han HJ, Yu T, Kim W-S, Im SH. 2016. Highly reproducible polyol synthesis for silver
321 nanocubes. J Cryst Growth 469:48-53.
- 322 12. da Silva AGM, Rodrigues TS, Wang J, Yamada LK, Alves T V., Ornellas FR, Ando RA,
323 Camargo PHC. 2015. The Fault in Their Shapes: Investigating the Surface-Plasmon-Resonance-
324 Mediated Catalytic Activities of Silver Quasi-Spheres, Cubes, Triangular Prisms, and Wires.
325 Langmuir 31:10272–10278.
- 326 13. Park JS, Ahn E-Y, Park Y. 2017. Asymmetric dumbbell-shaped silver nanoparticles and
327 spherical gold nanoparticles green-synthesized by mangosteen (*Garcinia mangostana*) pericarp waste
328 extracts. Int J Nanomedicine 12:6895–6908.
- 329 14. Farooq S, Dias Nunes F, de Araujo RE. 2018. Optical properties of silver nanoplates and
330 perspectives for biomedical applications. Photonics Nanostructures - Fundam Appl 31:160–167.
- 331 15. Petri M V., Ando RA, Camargo PHC. 2012. Tailoring the structure, composition, optical
332 properties and catalytic activity of Ag–Au nanoparticles by the galvanic replacement reaction. Chem
333 Phys Lett 531:188–192.
- 334 16. An K, Hyeon T. 2009. Synthesis and biomedical applications of hollow nanostructures. Nano
335 Today 4:359–373.
- 336 17. Xia X, Wang Y, Ruditskiy A, Xia Y. 2013. 25th Anniversary Article: Galvanic Replacement:
337 A Simple and Versatile Route to Hollow Nanostructures with Tunable and Well-Controlled
338 Properties. Adv Mater 25:6313–6333.
- 339 18. Ivask A, ElBadawy A, Kaweeteerawat C, Boren D, Fischer H, Ji Z, Chang CH, Liu R,
340 Tolaymat T, Telesca D, Zink JI, Cohen Y, Holden PA, Godwin HA. 2014. Toxicity Mechanisms in
341 *Escherichia coli* Vary for Silver Nanoparticles and Differ from Ionic Silver. ACS Nano 8:374–386.
- 342 19. Mohamed El-Azizi M, Nour El Din S, El-Tayeb T, Abou Aisha K. 2016. In vitro and in vivo
343 antimicrobial activity of combined therapy of silver nanoparticles and visible blue light against
344 *Pseudomonas aeruginosa*. Int J Nanomedicine 1749.
- 345 20. Toh HS, Batchelor-McAuley C, Tschulik K, Compton RG. 2014. Chemical interactions
346 between silver nanoparticles and thiols: a comparison of mercaptohexanol against cysteine. Sci China

- 347 Chem 57:1199–1210.
- 348 21. Chugh H, Sood D, Chandra I, Tomar V, Dhawan G, Chandra R. 2018. Role of gold and silver
349 nanoparticles in cancer nano-medicine. *Artif Cells, Nanomedicine, Biotechnol* 46:1210–1220.
- 350 22. Wan C, Tai J, Zhang J, Guo Y, Zhu Q, Ling D, Gu F, Gan J, Zhu C, Wang Y, Liu S, Wei F,
351 Cai Q. 2019. Silver nanoparticles selectively induce human oncogenic γ -herpesvirus-related cancer
352 cell death through reactivating viral lytic replication. *Cell Death Dis* 10:392.
- 353 23. Azizi M, Ghourchian H, Yazdian F, Bagherifam S, Bekhradnia S, Nyström B. 2017. Anti-
354 cancerous effect of albumin coated silver nanoparticles on MDA-MB 231 human breast cancer cell
355 line. *Sci Rep* 7:5178.
- 356 24. Jing Z-W, Luo M, Jia Y-Y, Li C, Zhou S-Y, Mei Q-B, Zhang B-L. 2018. Anti-*Helicobacter*
357 *pylori* effectiveness and targeted delivery performance of amoxicillin-UCCs-2/TPP nanoparticles
358 based on ureido-modified chitosan derivative. *Int J Biol Macromol* 115:367–374.
- 359 25. Arif M, Dong Q-J, Raja MA, Zeenat S, Chi Z, Liu C-G. 2018. Development of novel pH-
360 sensitive thiolated chitosan/PMLA nanoparticles for amoxicillin delivery to treat *Helicobacter pylori*.
361 *Mater Sci Eng C* 83:17–24.
- 362 26. Kravets V, Almemar Z, Jiang K, Culhane K, Machado R, Hagen G, Kotko A, Dmytruk I,
363 Spendier K, Pinchuk A. 2016. Imaging of Biological Cells Using Luminescent Silver Nanoparticles.
364 *Nanoscale Res Lett* 11:30.
- 365 27. Ardini M, Huang J-A, Sánchez CS, Mousavi MZ, Caprettini V, Maccaferri N, Melle G,
366 Bruno G, Pasquale L, Garoli D, De Angelis F. 2018. Live Intracellular Biorthogonal Imaging by
367 Surface Enhanced Raman Spectroscopy using Alkyne-Silver Nanoparticles Clusters. *Sci Rep*
368 8:12652.
- 369 28. Qing Y, Cheng L, Li R, Liu G, Zhang Y, Tang X, Wang J, Liu H, Qin Y. 2018. Potential
370 antibacterial mechanism of silver nanoparticles and the optimization of orthopedic implants by
371 advanced modification technologies. *Int J Nanomedicine Volume* 13:3311–3327.
- 372 29. Prasher P, Singh M, Mudila H. 2018. Silver nanoparticles as antimicrobial therapeutics:
373 current perspectives and future challenges. *3 Biotech* 8:411.
- 374 30. Lyczak JB, Cannon CL, Pier GB. 2002. Lung Infections Associated with Cystic Fibrosis. *Clin*

375 Microbiol Rev 15:194–222.

376 31. Vincent J-L. 2003. Nosocomial infections in adult intensive-care units. Lancet 361:2068–
377 2077.

378 32. Lee DG, Urbach JM, Wu G, Liberati NT, Feinbaum RL, Miyata S, Diggins LT, He J, Saucier
379 M, Déziel E, Friedman L, Li L, Grills G, Montgomery K, Kucherlapati R, Rahme LG, Ausubel FM.
380 2006. Genomic analysis reveals that *Pseudomonas aeruginosa* virulence is combinatorial. Genome
381 Biol 7:R90.

382 33. Stover CK, Pham XQ, Erwin AL, Mizoguchi SD, Warren P, Hickey MJ, Brinkman FS,
383 Hufnagle WO, Kowalik DJ, Lagrou M, Garber RL, Goltry L, Tolentino E, Westbrook-Wadman S,
384 Yuan Y, Brody LL, Coulter SN, Folger KR, Kas A, Larbig K, Lim R, Smith K, Spencer D, Wong
385 GK, Wu Z, Paulsen IT, Reizer J, Saier MH, Hancock RE, Lory S, Olson M V. 2000. Complete
386 genome sequence of *Pseudomonas aeruginosa* PAO1, an opportunistic pathogen. Nature 406:959–64.

387 34. Lister PD, Wolter DJ, Hanson ND. 2009. Antibacterial-Resistant *Pseudomonas aeruginosa*:
388 Clinical Impact and Complex Regulation of Chromosomally Encoded Resistance Mechanisms. Clin
389 Microbiol Rev 22:582–610.

390 35. Chairat S, Ben Yahia H, Rojo-Bezares B, Sáenz Y, Torres C, Ben Slama K. 2019. High
391 prevalence of imipenem-resistant and metallo-beta-lactamase-producing *Pseudomonas aeruginosa* in
392 the Burns Hospital in Tunisia: detection of a novel class 1 integron. J Chemother 31:120–126.

393 36. Erol S, Altoparlak U, Akcay MN, Celebi F, Parlak M. 2004. Changes of microbial flora and
394 wound colonization in burned patients. Burns 30:357–361.

395 37. Jugmohan B, Loveland J, Doedens L, Moore RL, Welthagen A, Westgarth-Taylor CJ. 2016.
396 Mortality in paediatric burns victims: A retrospective review from 2009 to 2012 in a single centre.
397 South African Med J 106:189.

398 38. Tacconelli E, Carrara E, Savoldi A, Harbarth S, Mendelson M, Monnet DL, Pulcini C,
399 Kahlmeter G, Kluytmans J, Carmeli Y, Ouellette M, Outtersson K, Patel J, Cavalieri M, Cox EM,
400 Houchens CR, Grayson ML, Hansen P, Singh N, Theuretzbacher U, Magrini N, Aboderin AO, Al-
401 Abri SS, Awang Jalil N, Benzonana N, Bhattacharya S, Brink AJ, Burkert FR, Cars O, Cornaglia G,
402 Dyar OJ, Friedrich AW, Gales AC, Gandra S, Giske CG, Goff DA, Goossens H, Gottlieb T, Guzman

403 Blanco M, Hryniewicz W, Kattula D, Jinks T, Kanj SS, Kerr L, Kieny M-P, Kim YS, Kozlov RS,
404 Labarca J, Laxminarayan R, Leder K, Leibovici L, Levy-Hara G, Littman J, Malhotra-Kumar S,
405 Manchanda V, Moja L, Ndoye B, Pan A, Paterson DL, Paul M, Qiu H, Ramon-Pardo P, Rodríguez-
406 Baño J, Sanguinetti M, Sengupta S, Sharland M, Si-Mehand M, Silver LL, Song W, Steinbakk M,
407 Thomsen J, Thwaites GE, van der Meer JW, Van Kinh N, Vega S, Villegas MV, Wechsler-Fördös A,
408 Wertheim HFL, Wesangula E, Woodford N, Yilmaz FO, Zorzet A. 2018. Discovery, research, and
409 development of new antibiotics: the WHO priority list of antibiotic-resistant bacteria and tuberculosis.
410 Lancet Infect Dis 18:318–327.

411 39. Fila G, Kawiak A, Grinholc MS. 2017. Blue light treatment of *Pseudomonas aeruginosa* :
412 Strong bactericidal activity, synergism with antibiotics and inactivation of virulence factors. Virulence
413 8:938–958.

414 40. Atta AM, Allohedan HA, El-Mahdy GA, Ezzat A-RO. 2013. Application of Stabilized Silver
415 Nanoparticles as Thin Films as Corrosion Inhibitors for Carbon Steel Alloy in 1 M Hydrochloric
416 Acid. J Nanomater 2013:1–8.

417 41. Acharya D, Singha KM, Pandey P, Mohanta B, Rajkumari J, Singha LP. 2018. Shape
418 dependent physical mutilation and lethal effects of silver nanoparticles on bacteria. Sci Rep 8:201.

419 42. Radzig MA, Nadtochenko VA, Koksharova OA, Kiwi J, Lipasova VA, Khmel IA. 2013.
420 Antibacterial effects of silver nanoparticles on gram-negative bacteria: Influence on the growth and
421 biofilms formation, mechanisms of action. Colloids Surfaces B Biointerfaces 102:300–306.

422 43. Guzman M, Dille J, Godet S. 2012. Synthesis and antibacterial activity of silver nanoparticles
423 against gram-positive and gram-negative bacteria. Nanomedicine Nanotechnology, Biol Med 8:37–
424 45.

425 44. Wypij M, Czarnecka J, Świecimska M, Dahm H, Rai M, Golinska P. 2018. Synthesis,
426 characterization and evaluation of antimicrobial and cytotoxic activities of biogenic silver
427 nanoparticles synthesized from *Streptomyces xinghaiensis* OF1 strain. World J Microbiol Biotechnol
428 34:23.

429 45. Sandri A, Ortombina A, Boschi F, Cremonini E, Boaretti M, Sorio C, Melotti P, Bergamini G,
430 Lleo M. 2018. Inhibition of *Pseudomonas aeruginosa* secreted virulence factors reduces lung

- 431 inflammation in CF mice. *Virulence* 9:1008–1018.
- 432 46. Rathinam P, Vijay Kumar HS, Viswanathan P. 2017. Eugenol exhibits anti-virulence
433 properties by competitively binding to quorum sensing receptors. *Biofouling* 33:624–639.
- 434 47. Thomann A, de Mello Martins AGG, Brengel C, Empting M, Hartmann RW. 2016.
435 Application of Dual Inhibition Concept within Looped Autoregulatory Systems toward Antivirulence
436 Agents against *Pseudomonas aeruginosa* Infections. *ACS Chem Biol* 11:1279–1286.
- 437 48. PROPST C, LUBIN L. 1979. Light-mediated Changes in Pigmentation of *Pseudomonas*
438 *aeruginosa* Cultures. *J Gen Microbiol* 113:261–266.
- 439 49. Muller M, Merrett ND. 2014. Pyocyanin Production by *Pseudomonas aeruginosa* Confers
440 Resistance to Ionic Silver. *Antimicrob Agents Chemother* 58:5492–5499.
- 441 50. Chairuangkitti P, Lawanprasert S, Roytrakul S, Aueviriyavit S, Phummiratch D, Kulthong K,
442 Chanvorachote P, Maniratanachote R. 2013. Silver nanoparticles induce toxicity in A549 cells via
443 ROS-dependent and ROS-independent pathways. *Toxicol Vitr* 27:330–338.
- 444 51. McShan D, Ray PC, Yu H. 2014. Molecular toxicity mechanism of nanosilver. *J Food Drug*
445 *Anal* 22:116–127.
- 446 52. Beer C, Foldbjerg R, Hayashi Y, Sutherland DS, Autrup H. 2012. Toxicity of silver
447 nanoparticles—Nanoparticle or silver ion? *Toxicol Lett* 208:286–292.
- 448 53. Choi O, Deng KK, Kim N-J, Ross L, Surampalli RY, Hu Z. 2008. The inhibitory effects of
449 silver nanoparticles, silver ions, and silver chloride colloids on microbial growth. *Water Res* 42:3066–
450 3074.
- 451 54. Lee W, Kim K-J, Lee DG. 2014. A novel mechanism for the antibacterial effect of silver
452 nanoparticles on *Escherichia coli*. *BioMetals* 27:1191–1201.
- 453 55. Saha K, Bajaj A, Duncan B, Rotello VM. 2011. Beauty is Skin Deep: A Surface Monolayer
454 Perspective on Nanoparticle Interactions with Cells and Bio-macromolecules. *Small* 7:1903–1918.
- 455 56. Hsiao I-L, Hsieh Y-K, Wang C-F, Chen I-C, Huang Y-J. 2015. Trojan-Horse Mechanism in
456 the Cellular Uptake of Silver Nanoparticles Verified by Direct Intra- and Extracellular Silver
457 Speciation Analysis. *Environ Sci Technol* 49:3813–3821.
- 458 57. Yuan Y-G, Peng Q-L, Gurunathan S. 2017. Effects of Silver Nanoparticles on Multiple Drug-

- 459 Resistant Strains of *Staphylococcus aureus* and *Pseudomonas aeruginosa* from Mastitis-Infected
460 Goats: An Alternative Approach for Antimicrobial Therapy. *Int J Mol Sci* 18:569.
- 461 58. Liao S, Zhang Y, Pan X, Zhu F, Jiang C, Liu Q, Cheng Z, Dai G, Wu G, Wang L, Chen L.
462 2019. Antibacterial activity and mechanism of silver nanoparticles against multidrug-resistant
463 *Pseudomonas aeruginosa*. *Int J Nanomedicine* Volume 14:1469–1487.
- 464 59. Siddiqi KS, Husen A, Rao RAK. 2018. A review on biosynthesis of silver nanoparticles and
465 their biocidal properties. *J Nanobiotechnology* 16:14.
- 466 60. Quinteros MA, Cano Aristizábal V, Dalmaso PR, Paraje MG, Páez PL. 2016. Oxidative
467 stress generation of silver nanoparticles in three bacterial genera and its relationship with the
468 antimicrobial activity. *Toxicol Vitr* 36:216–223.
- 469 61. Dwyer DJ, Belenky PA, Yang JH, MacDonald IC, Martell JD, Takahashi N, Chan CTY,
470 Lobritz MA, Braff D, Schwarz EG, Ye JD, Pati M, Vercruyse M, Ralifo PS, Allison KR, Khalil AS,
471 Ting AY, Walker GC, Collins JJ. 2014. Antibiotics induce redox-related physiological alterations as
472 part of their lethality. *Proc Natl Acad Sci* 111:E2100–E2109.
- 473 62. Baffou G, Quidant R. 2014. Nanoplasmonics for chemistry. *Chem Soc Rev* 43:3898.
- 474 63. Zhang D, Wang J. 2017. In Situ Photoactivated Plasmonic Ag₃PO₄@silver as a Stable
475 Catalyst With Enhanced Photocatalytic Activity Under Visible Light. *Mater Res* 20:702–711.
- 476 64. Gao L, Liu R, Gao F, Wang Y, Jiang X, Gao X. 2014. Plasmon-Mediated Generation of
477 Reactive Oxygen Species from Near-Infrared Light Excited Gold Nanocages for Photodynamic
478 Therapy in Vitro. *ACS Nano* 8:7260–7271.
- 479 65. da Silva AGM, Rodrigues TS, Correia VG, Alves T V., Alves RS, Ando RA, Ornellas FR,
480 Wang J, Andrade LH, Camargo PHC. 2016. Plasmonic Nanorattles as Next-Generation Catalysts for
481 Surface Plasmon Resonance-Mediated Oxidations Promoted by Activated Oxygen. *Angew Chemie*
482 128:7227–7231.
- 483 66. de Miguel I, Prieto I, Albornoz A, Sanz V, Weis C, Turon P, Quidant R. 2019. Plasmon-
484 Based Biofilm Inhibition on Surgical Implants. *Nano Lett* 19:2524–2529.
- 485 67. Zharov VP, Mercer KE, Galitovskaya EN, Smeltzer MS. 2006. Photothermal
486 Nanotherapeutics and Nanodiagnostics for Selective Killing of Bacteria Targeted with Gold

487 Nanoparticles. *Biophys J* 90:619–627.

488 68. Pihl M, Bruzell E, Andersson M. 2017. Bacterial biofilm elimination using gold nanorod

489 localised surface plasmon resonance generated heat. *Mater Sci Eng C* 80:54–58.

490 69. He D, Jones AM, Garg S, Pham AN, Waite TD. 2011. Silver Nanoparticle–Reactive Oxygen

491 Species Interactions: Application of a Charging–Discharging Model. *J Phys Chem C* 115:5461–5468.

492 70. He D, Garg S, Waite TD. 2012. H₂O₂-Mediated Oxidation of Zero-Valent Silver and

493 Resultant Interactions among Silver Nanoparticles, Silver Ions, and Reactive Oxygen Species.

494 *Langmuir* 28:10266–10275.

495 71. Lee PC, Meisel D. 1982. Adsorption and surface-enhanced Raman of dyes on silver and gold

496 sols. *J Phys Chem* 86:3391–3395.

497

498 **Legends to Figures**

499 **Figure 1.** Characterization of AgNPs. (a) Representative TEM and HRTEM (inset)

500 micrographs of citrate-coated AgNPs with an average diameter of 20 ± 3 nm. (b) Extinction

501 spectrum of AgNPs showing the SPR peak at 436 nm superposed with the LED floodlight

502 emission spectrum. The floodlight emission has a maximum intensity at 448 nm, with no

503 measurable emission from 190 to 406 nm.

504 **Figure 2.** Effect of AgNPs on *P. aeruginosa* survival. (a) Disc diffusion assay: Paper discs

505 containing each 10 μ L of 0, 10, 15, 20, 25 or 30 μ g/mL AgNPs were placed on Mueller-

506 Hinton plates spread with bacteria and incubated overnight under dark conditions. (b) Effect

507 of light on the bactericidal effect of AgNPs. Discs containing 10 μ g/mL AgNPs were placed

508 over *P. aeruginosa* lawns in the absence (left side) or presence (right side) of light.

509 **Figure 3.** Combined effect of light and AgNPs on bacterial viability. Bacteria were grown in

510 MH medium containing 1X MIC AgNPs (a), or 2X MIC AgNPs (b), in the absence (black) or

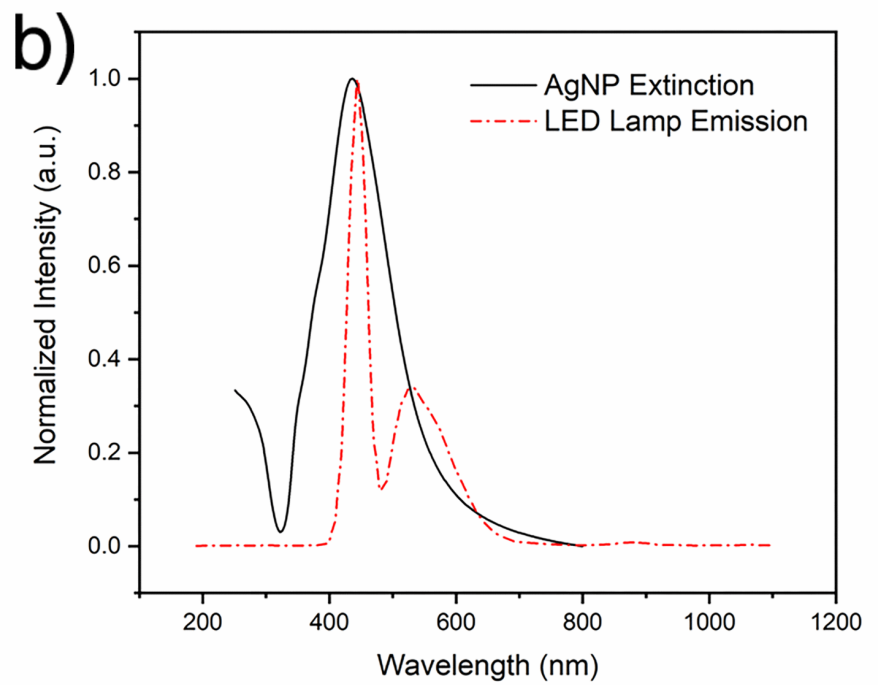
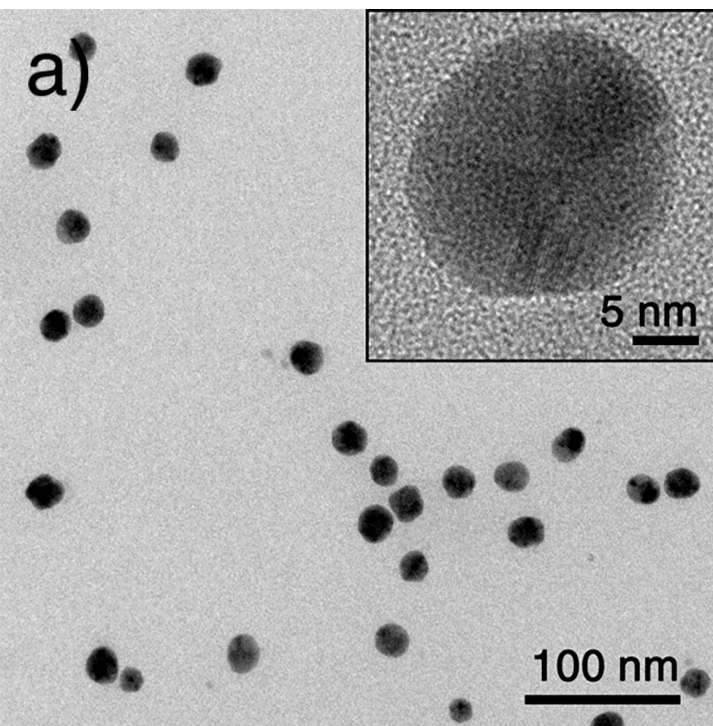
511 presence (white) of light. Aliquots of 100 μ L were withdrawn at 0, 15, 30 and 60 minutes to

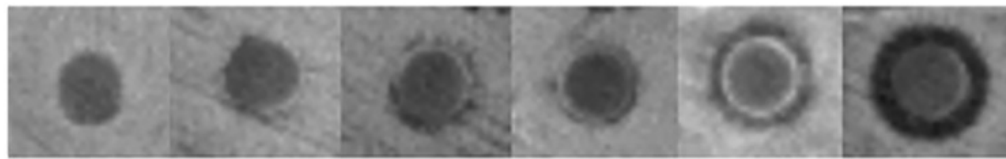
512 determine bacterial survival. The initial number of cells in all experiments was 1.64×10^5
513 CFU/mL. Each bar represents the mean \pm SD of 12 independent cultures. * $p < 0.05$

514 **Figure 4.** Light increases intracellular ROS generation in *P. aeruginosa* treated with AgNPs.
515 Bacteria were exposed for 1 hour to 10 $\mu\text{g/mL}$ AgNPs in the absence or presence of light.
516 Fluorescence intensities of DCFH-DA were measured by flow cytometry. Each point
517 represents the mean \pm SD of 3 independent cultures. * denotes statistical significance with $p <$
518 0.05.

519 **Figure 5.** Concentration of silver ions released by AgNPs through a dialysis membrane over
520 time in the presence (blue color) or absence of light (white color), respectively. A known
521 amount of AgNPs was added to a tightly closed dialysis membrane and the system was
522 submerged in distilled water under magnetic stirring. (a) Analysis of Ag^+ content by ICP-
523 OES. (b) Schematic representation of the dialysis method used to quantify silver ions.

524 **Figure 6.** Effect of light on bacteria growing in Mueller-Hinton medium. Bacterial growth
525 rate was determined by growing cells under dark or light conditions in MH medium and
526 measuring the number of colony forming units (CFU/mL) at different time points.





(-) 10 15 20 25 30

Concentration in $\mu\text{g/mL}$

a)

